

Electric-field-induced structural changes in KH_2PO_4 at room temperature and at 167 K

S. J. van Reeuwijk, A. Puig-Molina, and H. Graafsma*

European Synchrotron Radiation Facility, 6, rue Jules Horowitz, 38043 Grenoble, France

(Received 22 February 2001; revised manuscript received 7 May 2001; published 11 September 2001)

In this paper we report on the electric-field-induced changes in the structure of KH_2PO_4 (KDP) at two different temperatures determined by x-ray diffraction. One data set was measured at room temperature and the other at 167 K, significantly closer to the phase transition temperature of 122 K. The induced structural changes were determined from the measured changes in the integrated x-ray-diffraction intensities by means of a least-squares refinement. As expected, the structural changes induced at room temperature are enhanced when approaching T_C . The structural changes include the shifts of the atoms and the ordering of the hydrogen. At 167 K and in the presence of an electric field of 4×10^6 V/m parallel to the c axis, the P atom is displaced by $29(2) \times 10^{-4}$ Å along the c axis, and a redistribution of the hydrogen over the two formerly equivalent sites in the hydrogen bond takes place. The site towards which the P atom moves is decreased in occupancy in favor of the other by an amount of 1.4(5)%. The distortion of the oxygen framework is marginal. The induced structural changes in KDP are compared to those induced in its deuterated isomorph KD_2PO_4 (DKDP), which we measured previously [van Reeuwijk *et al.*, Phys. Rev. B **62**, 6192 (2000)]. The features of the structural changes induced in KDP and in DKDP are very similar. The ratio of the two main structural changes, i.e., the ordering of the proton in the hydrogen bond to the shift of the phosphor atom, is, however, isotope specific. Our results show great similarities with the observed structural changes around T_C [Nelmes *et al.*, J. Phys. C **18**, L711 (1985)].

DOI: 10.1103/PhysRevB.64.134105

PACS number(s): 77.84.Fa, 77.80.Bh, 77.65.Bn

I. INTRODUCTION

The studies of the influence of an external electric field on crystals have mainly been limited to macroscopic effects. With the development of powerful synchrotron sources, it became feasible to study the electric-field-induced changes at the atomic level by using x-ray diffraction,^{1,2} with the objective to gain a better insight into properties like piezoelectricity. Since the induced relative changes in diffracted intensity $\Delta I/I$ are on the order of 0.1%, a very suitable detection method is the modulation-demodulation technique.¹⁻³ A disadvantage of this technique is that it is restricted to the use of point detectors, resulting in long data collection times. Recently we have shown that a two-dimensional detector in combination with an incident-beam chopper can speed up the x-ray-diffraction experiment by one order of magnitude without degrading the data quality.⁴ This increase in data collection speed offers the possibility to study the influence of several external parameters (like temperature) on the induced structural changes.

Potassium dihydrogen phosphate (KDP) and its deuterated isomorph (DKDP) are well-known and extensively studied crystals undergoing ferroelectric phase transitions. Upon complete deuteration T_C changes from 122 to 229 K. This very large isotope effect was the subject of many theoretical and experimental studies aiming to reveal the role of the H/D in the process of the phase transition. Both Slater⁵ and Takagi⁶ worked out a theory for the phase transition, based on statistical methods describing the arrangement of the protons in each of the four disordered hydrogen bonds connected to a given phosphate group. Another approach is to describe the system with an appropriate Hamiltonian, which can be a simple Ising model Hamiltonian in a transverse tunneling field.⁷⁻¹⁰ The static properties of this model can be

evaluated in the mean-field approximation, whereas the dynamic properties are evaluated in the random-phase approximation. The short-range correlations of the protons around a given phosphate group are only included in the (dynamic) four-particle cluster approximation.^{8,9} A wealth of diffraction and spectroscopic data is available and can be used to examine the different theoretical models. The pressure effects, for example, can only be correctly accounted for using the four-particle cluster approximation.^{11,12}

From neutron and x-ray-diffraction studies detailed information about the *average* structure is obtained. In the paraelectric phase the four hydrogen atoms connected to a given phosphate group move between their two equilibrium positions in the hydrogen bonds linking the phosphate group with its neighboring phosphate groups. Since diffraction only provides information about the average structure, the two positions in the hydrogen bond, and hence all the positions, are crystallographically equivalent equilibrium positions; see Fig. 1. The space group for (D)KDP in this paraelectric phase is $I\bar{4}2d$, and the cell parameters of KDP at room temperature are $a = 7.4521(4)$ Å and $c = 6.974(2)$ Å.¹³ Below the Curie temperature, in the ferroelectric phase (space group $Fdd2$), the motion of the hydrogen atoms freezes out and the structure orders. Neutron-diffraction studies showed that the ordering of the protons/deuterons into one of the two equilibrium sites is gradual and accompanied with displacements of the heavy atoms.¹⁴⁻¹⁷ Another important observation was the discontinuity of some of the temperature parameters across the phase transition. Hydrostatic high-pressure neutron-diffraction experiments were performed to study the influence of the hydrogen bond dimension on the crystal characteristics.^{14,18-20} We continued the approach of perturbing the system and determining the induced structural changes, and reported recently on the changes induced in

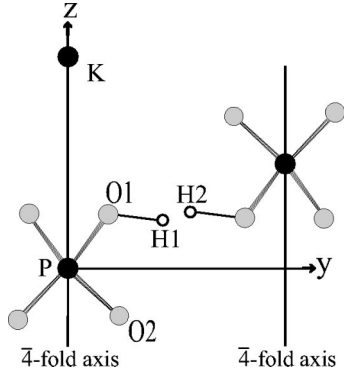


FIG. 1. Schematic representation of a part of the structure of KDP seen along the x axis. In the paraelectric phase the oxygen atoms, O1 and O2, are related to each other by the fourfold inversion axis parallel to the z axis, and the proton sites, H1 and H2, by a twofold rotation axis at $z = \frac{1}{8}$ perpendicular to the plane of view. The inclination of the $H \cdots H$ line with respect to the $z = \frac{1}{8}$ plane is exaggerated.

DKDP by an external electric field.^{2,4} The partial ordering of the structure was accompanied with displacements of the heavy atoms, similar to what Nelmes and co-workers found a few degrees below the Curie temperature.

In the paraelectric phase the crystal is piezoelectric. The piezoelectric tensor relates the externally applied electric field to the induced strain in the crystal. For KDP and DKDP the interesting tensor element is d_{36} , which means that by applying an external electric field along the c axis of the crystal, a change in γ angle is induced. By changing the γ angle, the space group changes from tetragonal $I\bar{4}2d$ to orthorhombic $Fdd2$, similar to cooling below T_C . In the case of DKDP we observed that, upon application of an external electric field parallel to the c axis, not only is the change of space group similar to cooling below T_C , but also the ordering of the structure and the displacement of the phosphor atom, which are the main structural changes.^{2,4} However, the size of the electric-field-induced changes is much smaller than the size of the changes induced by cooling.

The piezoelectric constant d_{36} is strongly temperature dependent and shows an anomaly at the phase-transition temperature.^{21–23} The temperature dependence can be described by a Curie-Weiss law,²²

$$d_{36} = d_{36}^0 + \frac{B}{T - T_C}. \quad (1)$$

For both KDP and DKDP we² observed that the piezoelectric constant obeys this Curie-Weiss law, and that the temperature-independent constant d_{36}^0 can be neglected even at room temperature. Equation (1) implies that, when approaching T_C at constant electric field, the deformation of the unit cell increases, and we also expect the induced changes in the structure to enhance.

The purpose of this paper is twofold. The first purpose is to identify the similarities and, more important, the differences in the electric-field-induced structural changes in

DKDP and in KDP. The second purpose is to observe the enhancement of the induced structural changes while approaching T_C . Hence we measured the electric-field-induced structural changes in KDP both at room temperature and at 167 K, much closer to the phase-transition temperature.

II. THEORY

When a static, or quasistatic, electric field is applied to a piezoelectric crystal, strains are developed in this crystal. This is the well-known converse piezoelectric effect. The elements of the strain tensor ϵ_{ij} are linearly related to the applied electric field by

$$\epsilon_{ij} = \sum_{k=1}^3 d_{kij} E_k, \quad (2)$$

where the summation is over the components of the electric field \mathbf{E} , and d_{kij} are the elements of the third-rank piezoelectric tensor.

In the case of an elastic, homogeneous, and infinitesimal deformation of the unit cell, it can be shown²⁴ that the Bragg angle of a reflection will be changed by an amount given by

$$\begin{aligned} \Delta\theta &= -\tan\theta \sum_{i=1}^3 \sum_{j=1}^3 h_i h_j \epsilon_{ij} \\ &= -\mathbf{E} \tan\theta \sum_{k=1}^3 \sum_{i=1}^3 \sum_{j=1}^3 e_k h_i h_j d_{kij}, \end{aligned} \quad (3)$$

where e_k and h_i are the components of the direction cosines of the electric field and the diffraction vector, respectively.

In general, the displacement of a particle, be it an atom, an ion, or a whole molecule, in the unit cell may be written as the sum of two contributions.^{1,25} The first contribution is due to the change in cell parameters, while keeping the fractional coordinates of the particle unchanged. It describes an elastic deformation, and is referred to as the *elastic* or *external* strain. In the case of ionic or atomic solids with no polyatomic units, the structure factor of reflection \mathbf{H} ,

$$F_{\mathbf{H}} = \sum_j f_j \exp(2\pi i \mathbf{H} \cdot \mathbf{x}_j) T_j, \quad (4)$$

only changes through small changes in the atomic scattering factors f_j , via a change in $\sin\theta/\lambda$, and possible changes in the temperature factors T_j . The summation in Eq. (4) runs over the individual atoms, which are located at the unchanged fractional coordinates \mathbf{x}_j . In the case of crystals consisting of rigid, polyatomic units, e.g., molecules, a change in the cell dimensions will not change the fractional coordinates of the center-of-mass of the polyatomic unit, but will change the fractional coordinates of the constituents of the polyatomic unit. Since the changes in fractional coordinates enter into the exponent of Eq. (4), the changes in structure factor are larger than for ionic or atomic solids.

The second contribution is the displacement of each particle *within* a (deformed) unit cell, and corresponds to changes in the fractional coordinates. This contribution is referred to as the *internal* strain. In crystals consisting of

polyatomic units, an electric field can induce a deformation or reorientation of the polyatomic units itself, leading to changes in fractional coordinates. Again, these changes enter into the exponent of Eq. (4) and significantly affect the structure factor.

Finally, the induced changes in the deformation density (polarization of the electron density) will lead to a change in the atomic scattering factors f_j and a corresponding change in the structure factor. This effect is expected to be smaller than the effect of the changes in fractional coordinates, and in any case mainly affects the low order reflections. Consequently, we do not consider this effect and focus on the changes in fractional coordinates of the individual atoms, taking into account the cell deformation.

III. EXPERIMENT

The measurements were carried out at the High Energy beamline ID15C of the European Synchrotron Radiation Facility using a wavelength of 0.32 Å. The c -cut single crystal of KDP (supplier MolTech GmbH, Berlin, Germany) used for the experiment at room temperature measured $a \times b \times c = 10 \times 10 \times 0.3$ mm³. Aluminum electrodes were evaporated on the optically polished faces of the crystal, perpendicular to the crystallographic c axis. The dimensions of the electrodes were slightly smaller than the faces of the crystal in order to prevent discharge through the air.

The quality of this sample was first tested by measuring the induced shifts of several $hh0$ reflections. In the case of (D)KDP and considering only $hh0$ reflections, the induced change of Bragg angle, given in Eq. (3), can be simplified to

$$\Delta \theta_{hh0} = -E_{\parallel c} \frac{d_{36}}{2} \tan \theta. \quad (5)$$

Once the shifts of several $hh0$ reflections are measured, the piezoelectric constant d_{36} can easily be determined.²⁶ The shifts can readily be measured with a point detector using the conventional modulation-demodulation technique.^{2,3} The recorded step scans contain two profiles, one for each direction of the electric field. The shift between the two profiles was determined using an algorithm based on the linear Pearson correlation coefficient. Figure 2 shows the measured shifts $\Delta \theta$ as function of $\tan \theta$. From Fig. 2 and using Eq. (5), d_{36} was found to be 21(2) pC/N, in good agreement with values found in the literature [20.9 pC/N].^{2,21} This indicates that the quality of the crystal is good and that the electric field is constant throughout the crystal.

Subsequently, the electric-field-induced changes in integrated intensities, related to the structural changes, were measured using a charge-coupled device (CCD) detector (16 bit Princeton Instruments ST130 camera with a Peltier-cooled 1152 × 1242 chip) optically coupled to an x-ray image intensifier. A schematic representation of the setup is given in Fig. 3. In the following a short description of the setup and the data collection strategy is given; more details can be found elsewhere.⁴

In order to prevent charge accumulation underneath the electrodes, which would result in a decreased electric-field

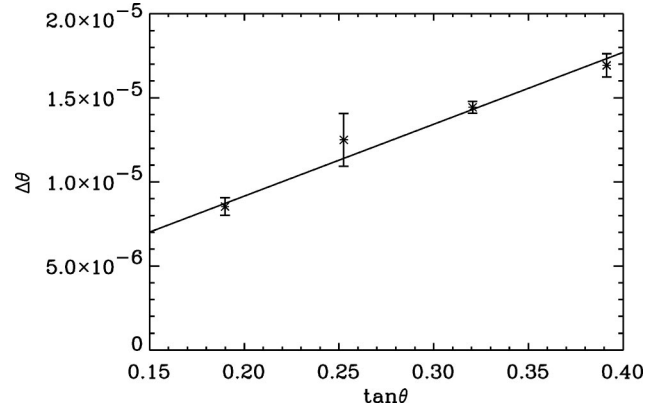


FIG. 2. The shift $\Delta \theta$ in radians of the (6 6 0), (8 8 0), (10 10 0), and (12 12 0) versus $\tan \theta$. Each of the reflections was measured several times, and the error bars were calculated from the spread in the data.

strength inside the crystal, the electric field is modulated with a frequency high enough to avoid charge buildup, and low enough to consider the electric field quasistatic. The relative long readout time of the CCD does not permit to demodulate the detector signal as is done with the conventional modulation-demodulation technique. By introducing a chopper in the incident beam and synchronizing it with the modulation of the electric field, it is possible to expose only with the electric field in a specific direction. After recording an image with the electric field in one direction, the synchronization is changed such that the next image is recorded with the electric field in the opposite direction. During exposure, the sample is oscillated around the spindle axis. Since the incident beam is chopped, the Bragg peaks are chopped as well and the recorded intensities come from slices of the Bragg peaks only. Simple simulations showed that under normal experimental conditions five chops per FWHM (full width at half maximum) are sufficient for a reliable determination of $\Delta I/I$.⁴

The applied electric field had an amplitude of 2.0×10^6 V/m and was switched with 113 Hz. The crystal was rotated with 0.2° s^{-1} , yielding about 15 chops per FWHM. Data were collected using 6° oscillations with 1° overlap at each side. The spindle axis was vertical and along the crystallographic a axis. Three of these ranges were collected around $\phi = 0^\circ$, where the c axis was parallel to the incident beam. Four of these ranges were collected around $\phi = 180^\circ$, three of which are symmetry related to the ranges collected around $\phi = 0^\circ$. Since the induced changes in the integrated

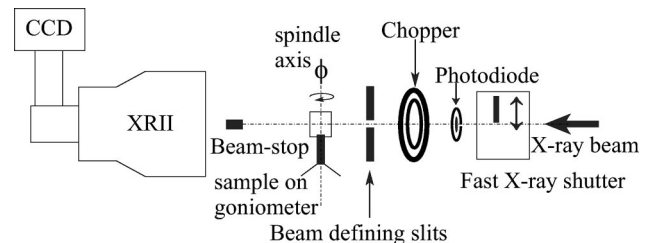


FIG. 3. Schematic representation of the experimental setup.

intensities are small, $\Delta I/I$ on the order of 0.1%, repetitive measurements were required to obtain sufficient accuracy. For each oscillation range around 200 images were taken for both states of the electric field. An acquisition with the electric field “positive” was followed by two acquisitions with the electric field “negative,” and one more with the electric field positive in order to obtain the same average incident-beam intensity for the two states of the electric field. The incident beam intensity was monitored with a silicon photodiode.

Since the input screen of the image intensifier is convex with respect to the sample, significant spatial distortions are introduced into the images. Before measuring the electric-field-induced changes in integrated intensity, the spatial distortion was calibrated using a standard technique.²⁷ The recorded images were online corrected for the spatial distortion.

For the experiment at low temperature a cryojet from Oxford Instruments was installed. In this experiment we used a sample that measured $a \times b \times c = 3 \times 3 \times 0.3$ mm³, which is slightly smaller than the cross section of the cold stream. Since the cold stream blew from above, the sample was placed with the spindle axis horizontal (along the crystallographic a axis) such that ice formation on the goniometer head and on the crystal was minimal. The amplitude and frequency of the applied electric field were identical to the data collection at room temperature. Three 6° oscillation ranges were collected around $\phi = 0^\circ$, where the c axis was parallel to the incident beam. Three symmetry related oscillation ranges were collected around $\phi = 180^\circ$.

Still at low temperature, the induced shifts of several $hh0$ reflections were measured with the point detector using the conventional modulation-demodulation technique. These data were used to determine the piezoelectric constant d_{36} , which was found to be 78(4) pC/N. From the temperature dependence of the d_{36} ,² the temperature of the sample was estimated to be 45 K above T_C , i.e., 167 K.

IV. DATA TREATMENT AND RESULTS

The orientation of the sample as well as the cell parameters were known, consequently some of the low-order reflections were easily indexed by inspection. With this information it was straightforward to index the remaining reflections with the DENZO package.²⁸

Subsequently, the integrated intensities of the diffraction spots were determined. First the images were corrected for the dark-current intensity, hot pixels, and cosmic rays. Then an integration box was defined around each diffraction spot. The outermost pixels were used to determine and subtract the background. The integrated intensity was then determined by summing over all the pixels in the integration box. Previous work on DKDP showed that this box-integration method was accurate enough to determine the induced changes in the structure,⁴ even though integration methods using profile fitting and/or optimization of the integration box are expected to yield even more accurate results.²⁹ Spots containing saturated pixels were not considered. The integrated intensities were scaled with the incoming beam monitor. For each re-

flexion the $\Delta I/I$ was calculated from two corresponding (consecutive) images as follows

$$\dots, \underbrace{\mathbf{E}_{pos}^i, \mathbf{E}_{neg}^i}_{\Delta I/I^i}, \underbrace{\mathbf{E}_{neg}^{i+1}, \mathbf{E}_{pos}^{i+1}}_{\Delta I/I^{i+1}}, \dots, \quad (6)$$

where i is the image number. All the $\Delta I/I^i$'s were averaged to obtain the $\Delta I/I$ for that reflection. The spread in the $\Delta I/I^i$'s was used to calculate the uncertainty in $\Delta I/I$. Reflections for which the $\Delta I/I^i$ showed a clear drift were rejected from further analyses. Most likely these reflections were partially recorded.

The program SORTAV (Ref. 30) was used to merge and sort the data, yielding, for the room-temperature data, a set of 60 unique reflections (in $Fdd2$), with an overall average measurement multiplicity of 2.6. The normalized root-mean-square deviation, $R2$, was 55%. The data at 167 K were merged and sorted to yield a set of 62 unique reflections, with an overall average measurement multiplicity of 4.0, and a $R2$ of 27%. The low-temperature data were of clearly better quality than the room-temperature data. A liable explanation is that the cold stream shielded the sample from influences of environmental fluctuations during the measurement of the low-temperature data.

The unique reflections were submitted to a refinement procedure. As stated in the introduction, the x-ray-diffraction experiment only gives the time and space averaged structure. Consequently, the refinement procedure only gives the average induced changes in the structure. The cell parameters, fractional coordinates, and anisotropic temperature parameters of the paraelectric phase were taken from Tun,¹³ and transformed to space group $Fdd2$. The magnitude of the changes in cell parameters can easily be calculated from the known electric-field strength and the piezoelectric constant d_{36} . However, since the shifts of the diffraction peaks are too small to be measured with the image intensifier used, the assignment of a and b axes, and consequently the h and k Miller indices, cannot be made unambiguously. A point detector allows the simultaneous measurement of both the shift and intensity change of a reflection, and thus the unambiguous assignment of cell axes and Miller indices. Since it is expected that DKDP and KDP show similar behavior, we used previous data of DKDP, measured with a point detector,² to make the correct assignment of the a and b axes, and the h and k Miller indices. In conjunction with this cell change, the phosphate group was supposed to be a rigid unit and the fractional coordinates of the oxygen and hydrogen atoms were adapted accordingly. Subsequently, the fractional coordinates (the shifts of the atoms) were refined with a least-squares minimization procedure that uses SHELXL-93 (Ref. 31) to calculate the structure factors. The electric field destroys the symmetry relating the O1 and O2 atoms (the “upper” and “lower” oxygens in Fig. 1), resulting in two crystallographically independent oxygen atoms. All the free coordinates of the nonhydrogen atoms in space group $Fdd2$ were refined, i.e., the x , y , and z coordinates of the two oxygens and the z coordinate of the phosphor. Although the two oxygen atoms are crystallographically independent, the shifts of the two atoms are related by virtue of the linearity

TABLE I. Refined atomic parameters. The shifts are given in 10^{-4} Å, the changes in the occupancies in percent.

	Δx	Δy	Δz	Δ occupancy
KDP	T=RT	$R2^a=55\%$	$wR2^b=45\%$	
P			+8(1)	
O1	-0.7(6)	-0.3(6)	-21(12)	
O2	-0.3	+0.7	-21	
H1	-0.7	-0.3	-21	-0.8(8)
H2	-0.3	+0.7	-21	+0.8
KDP	T=167 K	$R2=27\%$	$wR2=27\%$	
P			+29(2)	
O1	+2.6(6)	+0.4(6)	+12(6)	
O2	+0.4	-2.6	+12	
H1	+2.6	+0.4	+12	-1.4(5)
H2	+0.4	-2.6	+12	+1.4
DKDP ^c	T=RT	$R2=25\%$	$wR2=37\%$	
P			+26(3)	
O1	+1.4(2)	+0.0(2)	+5(2)	
O2	+0.0	-1.4	+5	
H1	+1.4	+0.0	+5	-0.9(2)
H2	+0.0	-1.4	+5	+0.9
DKDP ^d	T=RT	$R2=23\%$	$wR2=25\%$	
P			+20.7(5)	
O1	+2.0(2)	+0.4(2)	+2(2)	
O2	+0.4	-2.0	+2	
H1	+2.0	+0.4	+2	-0.7(3)
H2	+0.4	-2.0	+2	+0.7

^aRoot-mean-square deviation of merging.

^bWeighted root-mean-square deviation of the refinement.

^cMeasured with the point detector (Ref. 2).

^dMeasured with the two-dimensional (2D) detector (Ref. 4).

of the piezoelectric effect: $\Delta x(O1) = -\Delta y(O2)$, $\Delta y(O1) = \Delta x(O2)$, and $\Delta z(O1) = \Delta z(O2)$. Since the two-fold axis relating the two sites of the proton in the hydrogen bond is also destroyed, the distribution of the proton over these two sites is another parameter to refine (the total occupancy of the two sites is restrained to 100%). The hydrogen atoms were assumed to follow the oxygen atoms they are attached to.

During both the refinement of the room-temperature data and the data at 167 K, five reflections were rejected as outliers. For the data set at 167 K, these outliers were all low order reflections and thus affected by changes in the deformation density which are not accounted for in the model. In the case of the room-temperature data some of the outliers were high-order reflections, illustrating that the data set at 167 K is of better quality than the data set at room temperature. For both data sets the refinement converged within three cycles, and the results are given in Table I. In that table we also listed the results on DKDP since careful inspection revealed that the a and b axes were interchanged in the refinement procedures reported previously,^{2,4} and thus the data were reanalyzed. The resulting structural changes for DKDP obviously changed sign, but the magnitude of the shifts was not affected significantly.

TABLE II. Values obtained for the ratios of the ordering over $\Delta z(P)$ and the polarization over the strain for KDP and DKDP.

	$\Delta \gamma$ (rad)	$\frac{\text{ord}^a}{\Delta z(P)} (\text{\AA}^{-1})$	$\frac{P_3}{\Delta \gamma} \left(\frac{\text{C}}{\text{cm}^2} \right)$
KDP RT	8.8×10^{-5}	b	$8(1) \times 10^{-4}$
KDP 167 K	31.2×10^{-5}	$9(3) \times 10^2$	$7.8(5) \times 10^{-4}$
DKDP ^c	15.5×10^{-5}	$7(3) \times 10^2$	$9(2) \times 10^{-4}$

^aThe order parameter is defined as $2 \times (\text{occupancy} - 50)\%$.

^bNot calculated since $\sigma(\Delta \text{occ})$ is too large.

^cCalculated from the 2D data.

Table I shows that the quality of the refinement of the KDP data at room temperature (RT) is significantly lower, in terms of R factors, than the refinement of the other data sets. At room temperature, the only significant structural change is $\Delta z(P)$. Refining only $\Delta z(P)$ hardly affects the statistics ($wR2 = 49\%$).

V. DISCUSSION

From Table I it is clear that the structural changes induced by an external electric field in KDP and in DKDP have the same tendency. The phosphor atom shifts along the c axis, and the proton (deuteron) orders into one of the previously equivalent sites. If the phosphor in Fig. 1 shifts towards the upper oxygens, the hydrogen (deuteron) orders away from the upper oxygens. The tetrahedra of oxygen atoms deform only marginally. These features are consistent with the structural changes induced by cooling below the phase-transition temperature measured by Nelmes *et al.*¹⁵

The data of Nelmes *et al.* show that when cooling below T_C the ratio of the order parameter [defined as $2 \times (\text{occupancy} - 50)\%$] to the shift of the phosphor atom has a constant value. For KDP this ratio is $9.1(3) \times 10^2 \text{\AA}^{-1}$. The electric-field-induced ordering of the proton in the hydrogen bond is not well determined for KDP at room temperature, as Table I shows, and can consequently not be used for a quantitative analysis. At 167 K, the ratio of the order parameter to the shift of the phosphor atom is $9(3) \times 10^2 \text{\AA}^{-1}$, see also Table II, in good agreement with the results from Nelmes.

As was stated in the Introduction, the electric-field-induced structural changes at room temperature are expected to enhance upon cooling, more precisely, they are expected to follow the induced change in γ angle. According to Jona and Shirane,²² the proportionality between the induced polarization and the strain is a fundamental property of piezoelectric crystals. The induced polarization can be calculated, in an approximate manner, from the refined structural changes assuming formal point charges. In the case of KDP the displacements of the oxygen atoms are not well determined. Furthermore, the ordering of the hydrogen bond is nearly perpendicular to the c axis and hardly contributes to the induced polarization. Consequently, the polarization (along c) is calculated from the shift of the phosphor atom only. The shear strain x_y is just $\Delta \gamma$, and can be calculated from the piezoelectric constant and the applied electric field strength.

The obtained fundamental ratio between the induced polarization and the strain is given in Table II. The ratio is not affected by a change in temperature, as was expected. This ratio can also be calculated from the relation between the polarization and the electric field

$$E = \alpha(T - T_C)P + \beta P^3 + \gamma P^5, \quad (7)$$

the Curie-Weiss law for the piezoelectric constant, Eq. (1), and the relation for the induced strain, Eq. (2). At both temperatures measured, Eq. (7) is dominated by its first term, resulting in a Curie-Weiss law for the polarization over the electric field. Combining all three equations yields

$$\frac{P_3}{x_y} = \frac{1}{\alpha B}. \quad (8)$$

Substituting the α from Kobayashi *et al.*³² and the B as determined in our previous paper,² the temperature-independent fundamental constant equals $8.0(1) \times 10^{-4}$ C/cm², in excellent agreement with the values given in Table II.

Similar calculations can be made for DKDP, and the results are listed in Table II. The data of Nelmes *et al.* indicate that the ratio of the order parameter to the shift of the phosphor atom is $7.4(1) \times 10^2 \text{ \AA}^{-1}$, which is in good agreement

with our result. The proportionality between the induced polarization and the strain is calculated from all the refined structural changes since for DKDP all the structural changes are well determined. The calculated value of $9(2) \times 10^{-4}$ C/cm² cannot be compared with the right-hand side of Eq. (8) since the α parameter for DKDP is, to our knowledge, not available in the literature. On the other hand, the ratio of the induced polarization to the strain equals the ratio of the dielectric susceptibility to the piezoelectric constant.²² The tabulated²¹ relative dielectric constant and the piezoelectric tensor element can be used to calculate the ratio between the susceptibility and the piezoelectric constant, and thus the fundamental ratio between the polarization and the strain. The accordingly calculated value is 9×10^{-4} C/cm² and agrees well with the experimentally determined value.

Summarizing, we can say that our electric-field-induced structural changes agree well with other experiments. The ratios of the order parameter over the shift of the phosphor atom, and of the induced polarization over the strain are isotope specific. The data from Nelmes *et al.* clearly show this for the ratio of the ordering over the shift of the phosphor atom. For the electric-field-induced structural changes the ratios appear to be isotope specific as well, but the difference between the ratios of the two isotopes is at the limit of the measurement accuracy.

*Author to whom correspondence should be addressed. Electronic address: graafsma@esrf.fr

¹H. Graafsma, A. Paturle, L. Wu, H.-S. Sheu, J. Majewski, G. Poorthuis, and P. Coppens, *Acta Crystallogr., Sect. A: Found. Crystallogr.* **A48**, 113 (1992).

²S.J. van Reeuwijk, A. Puig-Molina, and H. Graafsma, *Phys. Rev. B* **62**, 6192 (2000).

³A. Paturle, H. Graafsma, H.-S. Sheu, and P. Coppens, *Phys. Rev. B* **43**, 14 683 (1991).

⁴S.J. van Reeuwijk, V. Vonk, A. Puig-Molina, and H. Graafsma, *J. Appl. Crystallogr.* **33**, 1422 (2000).

⁵J.C. Slater, *J. Chem. Phys.* **9**, 16 (1941).

⁶Y. Takagi, *Proc. Phys. Math. Soc. Jpn.* **23**, 44 (1941).

⁷P.G. De Gennes, *Solid State Commun.* **1**, 132 (1963).

⁸R. Blinc, B. Žekš, and R.J. Nelmes, *Phase Transitions* **3**, 293 (1983).

⁹R. Blinc and B. Žekš, *Soft Modes in Ferroelectrics and Antiferroelectrics* (North-Holland, Amsterdam, 1974).

¹⁰R. Blinc and B. Žekš, *J. Phys. C* **15**, 4661 (1982).

¹¹R. Blinc and B. Žekš, *Helv. Phys. Acta* **41**, 701 (1968).

¹²I.V. Stasyuk, R.R. Levitskii, and A.P. Moina, *Phys. Rev. B* **59**, 8530 (1999).

¹³Z. Tun, R.J. Nelmes, W.F. Kuhs, and R.F.D. Stansfield, *J. Phys. C* **21**, 245 (1988).

¹⁴R.J. Nelmes, *Ferroelectrics* **71**, 87 (1987).

¹⁵R.J. Nelmes, W.F. Kuhs, C.J. Howard, J.E. Tibbals, and T.W. Ryan, *J. Phys. C* **18**, L711 (1985).

¹⁶B.C. Frazer and R. Pepinsky, *Acta Crystallogr.* **6**, 273 (1953).

¹⁷T. Kikuta, A. Onodera, T. Takama, M. Fujita, and H. Yamashita, *Ferroelectrics* **170**, 17 (1995).

¹⁸J.E. Tibbals, R.J. Nelmes, and G.J. McIntyre, *J. Phys. C* **15**, 37 (1982).

¹⁹M.I. McMahon, R.J. Nelmes, W.F. Kuhs, R. Dorwarth, R.O. Piltz, and Z. Tun, *Nature (London)* **348**, 317 (1990).

²⁰J.E. Tibbals and R.J. Nelmes, *J. Phys. C* **15**, L849 (1982).

²¹*Low Frequency Properties of Dielectric Crystals*, Landolt-Börnstein, New Series, Group III, Vol. 29, Pt. b (Springer-Verlag, Berlin, 1993).

²²F. Jona and G. Shirane, *Ferroelectric Crystals* (Pergamon, Oxford, 1962), Chap. III.

²³M.P. Zaitseva, Yu.I. Kokorin, A.M. Sysoev, and I.S. Rez, *Kristallografiya* **27**, 146 (1982) [*Sov. Phys. Crystallogr.* **27**, 86 (1982)].

²⁴G.R. Barsch, *Acta Crystallogr., Sect. A: Cryst. Phys., Diffraction, Theor. Gen. Crystallogr.* **A32**, 575 (1976).

²⁵M. Born and K. Huang, *Dynamical Theory of Crystal Lattices* (Oxford University Press, Oxford, 1954), p. 134.

²⁶H. Graafsma, *J. Appl. Crystallogr.* **25**, 372 (1992).

²⁷J.P. Moy, A.P. Hammersley, S.O. Svensson, A. Thompson, K. Brown, L. Claustre, A. Gonzalez, and S. McSweeney, *J. Synchrotron Radiat.* **3**, 1 (1996).

²⁸Z. Otwinowski and W. Minor, *Methods in Enzymology, Macromolecular Crystallography Vol. 276A*, edited by C. W. Carter and R. M. Sweet (Academic Press, New York, 1997), p. 307.

²⁹D. Bourgeois, D. Nurizzo, R. Kahn, and C. Cambillau, *J. Appl. Crystallogr.* **31**, 22 (1998).

³⁰R.H. Blessing, *J. Appl. Crystallogr.* **22**, 396 (1989).

³¹G. M. Sheldrick, SHELXL-93, Program for the Refinement of Crystal Structures (University of Göttingen, Germany, 1993).

³²J. Kobayashi, Y. Uesu, and Y. Enomoto, *Phys. Status Solidi B* **45**, 293 (1971).